A Numerical Investigation of Developing Flow in Curved Pipe

M.R.H. Nobari [1], Jalal Behzadi [2], Ali Asgarian [3]

[1] Associate Professor, E-mail: mrnobari@cic.aut.ac.ir
[2] Graduate Student, E-mail: j_behzadi@yahoo.com
[3] Graduate Student, E-mail: asgarian@gmail.com

Amirkabir University of Technology, Mechanical Engineering Department, 424 Hafez Ave.,
P.O. Box 15875-4413, Tehran, Iran

Keywords: Curved Pipe, Finite Difference, Entrance Length

Abstract. *Developing incompressible viscous flow in a curved pipe is numerically simulated by solving full Navier-Stokes equations in a toroidal coordinate system using second order finite difference discritization in space based on projection method. To get a physical pressure field, a staggered structured grid is used. The numerical results obtained here include a range of curvature ratios (the ratio of pipe radius to curvature radius, $\delta = a/R$) between 1 / 30 and 1/ 10 and the Reynolds numbers from 125 to 750. The numerical results are compared with available data to validate the accuracy of the code implemented. As a new contribution, a correlation is introduced to predict the entrance length as a function of curvature ratio and Reynolds number. It is observed that the entrance length increases with increasing Re and decreasing curvature ratio. Also pressure drop in axial direction is studied for various conditions.*

NOMENCLATURE

a	**pipe's radius**
B	a dimensionless variable, $B = 1 + \delta r \cos\phi$
D	pipe's diameter
L	fully developed length
m	number of grid intervals in r direction
n	number of grid intervals in ϕ direction
P'	pressure
P	dimensionless pressure, $P = \frac{P'}{\rho \bar{w}^2}$
q	number of grid intervals in θ direction
r'	first coordinate in Toroidal system
r	dimensionless first coordinate in Toroidal system, $r = r'/a$
R	radius of curvature
Re	Reynolds number, $\mathrm{Re} = \frac{a\bar{w}}{\upsilon}$
t'	time
t	dimensionless time, $t = \frac{t'\bar{w}}{a}$
u'	velocity component in r direction
u	dimensionless velocity component in r direction, $u = u'/\bar{w}$
v'	**velocity component in φ direction**
v	dimensionless velocity component in φ direction, $u = u'/\bar{w}$
V'	velocity vector
V	dimensionless velocity vector, $V = V'/\bar{w}$
w'	velocity component in θ direction
w	dimensionless velocity component in θ direction, $w = w'/\bar{w}$
x	first coordinate in Cartesian system
y	second coordinate in Cartesian system
z	third coordinate in Cartesian system
Greek Symbols	
δ	curvature ratio, $\delta = a/R$
ε_{fd}	criterion for fully developed length
ϕ	second coordinate in Toroidal system
θ	third coordinate in Toroidal system
Superscripts	
n	current time step
$*$	auxiliary time step

1 INTRODUCTION

Fluid flow in the entrance region of a curved pipe is of great importance to physiologists due to its relevance to the phenomena such as mixing of injected substance in the blood vessels to get more information about vessel diseases (atherosclerosis in arteries). In the industry, the flow in curved pipes encounters in heat exchangers, horizontal coils, turbine blade cooling systems and piping operations.

Most of the analyses of the fully developed flow in the curved pipes have been carried out on the assumption of loose curved pipes where the curvature ratio (δ) is small. Dean [1,2] has shown that in the small curvature ratios, the fluid flow depends only on a single non-dimensional parameter, i.e. Dean number. Patankar et al.[3] have studied the development of flow and temperature in a curved pipe with the poiseuille flow at the inlet. Soh and Berger [4] solved the associated governing equations using a finite difference method based on the artificial compressibility technique represented by Chorin. Agrawal et al.[5] in an experimental work have measured the axial and secondary flow velocities in the fully developed region by the laser-Doppler velocity-meter.

Kumar and Nigam[6] introduced a new device to improve the performance of heat exchangers based on the flow inversion by changing the direction of secondary flow in helically coiled tubes. Nobari and K. Gharali[7] have investigated the effects of internal fins on the flow and heat transfer inside rotating straight pipes and stationary curved pipes. Their numerical results that have been obtained using the finite volume method based on the SIMPLE algorithm show an optimum fin height about 0.8 of pipe radius.

In this article the flow development in a curved pipe is studied numerically using the finite difference method based on the projection algorithm to solve the full Navier-Stokes equations. Parabolic velocity profile is applied at the inlet to run the code at different values of curvature ratios and Reynolds numbers. Finally a correlation to predict the hydrodynamically fully developed entrance length is proposed in terms of curvature ratio and Reynolds number.

2 GOVERNING EQUATIONS

The geometry of the curved pipe is depicted in Fig. 1. At the inlet fully developed velocity profile of a straight pipe is used. Inside the curved pipe the axial profile deforms due to presence of centrifugal forces and gradually approaches to a new fully developed profile.

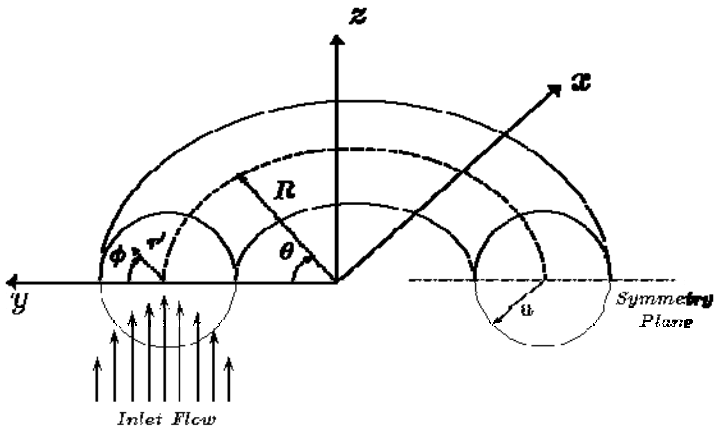

Figure 1. Geometry of the curved pipe

The vector form of the governing equations including continuity and momentum for a Newtonian incompressible fluid are

$$\begin{cases} \nabla \cdot V = 0 \\ \dfrac{\partial V}{\partial t} + (V \cdot \nabla)V + V\,(\nabla \cdot V) = -\nabla P + \dfrac{1}{\mathrm{Re}}\nabla^2 V \end{cases} \tag{1}$$

For convenience, the governing equations are written in the Toroidal coordinate system where the three corresponding components (r', ϕ, θ) are shown in Fig. 2. Since the Toroidal coordinate system is orthogonal and fully compatible with the geometry of the curved pipe, it facilitates the generation of a uniform structured orthogonal grid which is suitable in implementing finite difference discretization.

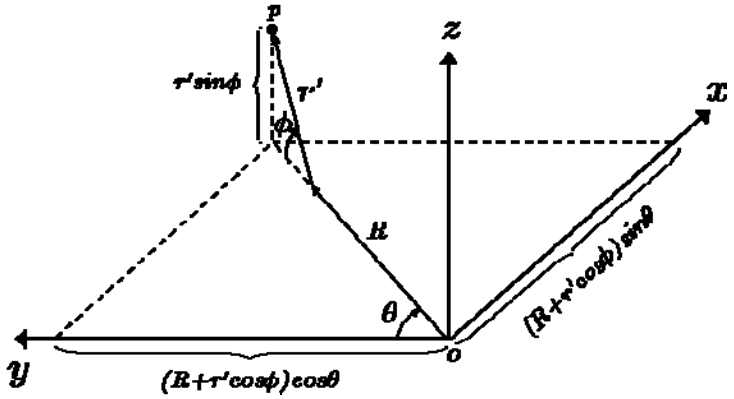

Figure 2. Toroidal coordinate system

Interdependence between Toroidal and Cartesian is as follows,

$$\begin{cases} x = (R + r'\cos\phi)\sin\theta \\ y = (R + r'\cos\phi)\cos\theta \\ z = r'\sin\phi \end{cases} \tag{2}$$

Making use of dimensionless vector form of the Navier-Stokes equation and also vector operators in an orthogonal curvilinear coordinate system[8], the dimensionless equations in the Toroidal system are

Continuity

$$\frac{\partial}{\partial r}(rBu) + \frac{\partial}{\partial \phi}(Bv) + \frac{\partial}{\partial \theta}(\delta r w) = 0 \tag{3}$$

r-momentum equation

$$\begin{aligned} &\frac{\partial u}{\partial t} + \frac{1}{rB}\left[\frac{\partial}{\partial r}(rBu^2) + \frac{\partial}{\partial \phi}(Buv) + \frac{\partial}{\partial \theta}(\delta ruw) - Bv^2 - \delta r\cos\phi w^2\right] = -\frac{\partial p}{\partial r} \\ &+ \frac{1}{\mathrm{Re}}\left\{\frac{1}{rB}\left[\frac{\partial}{\partial r}(rB\frac{\partial u}{\partial r}) + \frac{\partial}{\partial \phi}(\frac{B}{r}\frac{\partial u}{\partial \phi}) + \frac{\partial}{\partial \theta}(\frac{\delta^2 r}{B}\frac{\partial u}{\partial \theta})\right]\right. \\ &\left. - \frac{1}{r^2}(2\frac{\partial v}{\partial \phi} + u) + \frac{\delta\sin\phi v}{rB} + \frac{\delta^2\cos\phi}{B^2}(v\sin\phi - u\cos\phi - 2\frac{\partial w}{\partial \theta})\right\} \end{aligned} \tag{4}$$

φ-momentum equation

$$\begin{aligned} &\frac{\partial v}{\partial t} + \frac{1}{rB}\left[\frac{\partial}{\partial r}(rBuv) + \frac{\partial}{\partial \phi}(Bv^2) + \frac{\partial}{\partial \theta}(\delta r v w) + Buv + \delta r\sin\phi w^2\right] = -\frac{1}{r}\frac{\partial p}{\partial \phi} \\ &+ \frac{1}{\mathrm{Re}}\left\{\frac{1}{rB}\left[\frac{\partial}{\partial r}(rB\frac{\partial v}{\partial r}) + \frac{\partial}{\partial \phi}(\frac{B}{r}\frac{\partial v}{\partial \phi}) + \frac{\partial}{\partial \theta}(\frac{\delta^2 r}{B}\frac{\partial v}{\partial \theta})\right]\right. \\ &\left. + \frac{1}{r^2}(2\frac{\partial u}{\partial \phi} - v) - \frac{\delta\sin\phi u}{rB} - \frac{\delta^2\sin\phi}{B^2}(v\sin\phi - u\cos\phi - 2\frac{\partial w}{\partial \theta})\right\} \end{aligned} \tag{5}$$

θ-momentum equation

$$\frac{\partial w}{\partial t}+\frac{1}{rB}\left[\frac{\partial}{\partial r}(rB\,u\,w)+\frac{\partial}{\partial \phi}(B\,v\,w)+\frac{\partial}{\partial \theta}(\delta\,r w^{2})+\delta\,r w\,(u\cos\phi-v\,\sin\phi)\right]=-\frac{\delta}{B}\frac{\partial p}{\partial \theta}$$
$$+\frac{1}{\mathrm{Re}}\left\{\frac{1}{rB}\left[\frac{\partial}{\partial r}(rB\,\frac{\partial w}{\partial r})+\frac{\partial}{\partial \phi}(\frac{B}{r}\frac{\partial w}{\partial \phi})+\frac{\partial}{\partial \theta}(\frac{\delta^{2}r}{B}\frac{\partial w}{\partial \theta})\right]+\frac{2\delta^{2}}{B^{2}}(\frac{\partial u}{\partial \theta}\cos\phi-\frac{\partial v}{\partial \theta}\sin\phi-\frac{w}{2})\right\} \tag{6}$$

where, $B=1+\delta r\cos\phi$.

In the above equations, the body forces are neglected because of their small contribution. Due to the symmetry of the problem, only the upper-half of the pipe is considered. The boundary conditions applied are

- No-slip condition at the wall ($r'=a$ or $r=1$)

$$u=v=w=0. \tag{7}$$

- At the pipe entrance ($\theta=0$) there is only axial velocity obtained from fully developed solution of a straight pipe (parabolic profile),

$$u=v=0\ ,\ w=2\left(1-r^{2}\right). \tag{8}$$

- At the exit ($\theta=\pi$), fully developed conditions are assumed

$$\frac{\partial u}{\partial \theta}=\frac{\partial v}{\partial \theta}=\frac{\partial w}{\partial \theta}=0. \tag{9}$$

- At the symmetry boundaries ($\phi=0$ and $\phi=\pi$), the velocity component normal to these boundaries is zero and for the other components, Neumann condition is applied

$$v=0\ ,\ \frac{\partial u}{\partial \phi}=\frac{\partial w}{\partial \phi}=0. \tag{10}$$

3 NUMERICAL METHOD

Second order finite difference method in space is used to solve the equations numerically based on the projection algorithm as follows

$$\begin{cases}\nabla\cdot V^{n+1}=0\\ \dfrac{V^{n+1}-V^{n}}{\Delta t}+(V^{n}\cdot\nabla)V^{n}+\nabla P^{n+1}=\dfrac{1}{\mathrm{Re}}\nabla^{2}V^{n}\end{cases} \tag{11}$$

where the superscript *n* represents the *n*th time step. Using an auxiliary velocity represented as V^{*}, momentum equation is split into the following equations

$$\frac{V^{*}-V^{n}}{\Delta t}+(V^{n}\cdot\nabla)V^{n}=\frac{1}{\mathrm{Re}}\nabla^{2}V^{n} \tag{12}$$

$$\frac{V^{n+1}-V^{*}}{\Delta t}+\nabla P^{n+1}=0 \tag{13}$$

It is obvious that addition of Eqs. (12) and (13) leads to the original equation. Taking divergence of Eq. (13) and imposing the continuity at the new time step, Poisson equation for the pressure field is obtained

$$\nabla^{2}P^{n+1}=\frac{1}{\Delta t}\nabla\cdot V^{*} \tag{14}$$

Eqs. (12), (13), and (14) must be solved to determine the velocities and pressure. In order to discretize the equations, uniform grid in the Toroidal coordinate system which is suitable for the finite difference method is used. As mentioned above, due to symmetry, it is enough only to consider the upper half of the pipe which is

defined as $0 \le r' \le a$, $0 \le \phi \le \pi$ *and* $0 \le \theta \le \pi$. Therefore, this region is divided into *m*, *n*, and *q* equal intervals in the three directions of $r, \phi,$ and θ respectively.

$$\Delta r' = \frac{a}{m} \quad , \quad \Delta\varphi = \frac{\pi}{n} \quad , \quad \Delta\theta = \frac{\pi}{q} \tag{15}$$

A sample of the generated grid is illustrated in Fig. 3. Analysis of the numerical results for several grids of various sizes is carried out to show the independence of the code implemented. Most of the results presented here are obtained using a grid size of $m = 15$, $n = 30$ and $q = 72$.

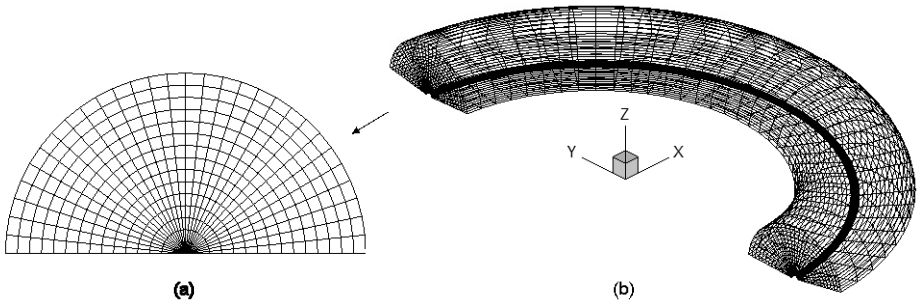

Figure 4. (a) Cross section of grid (b) 3D grid

In order to obtain a physical pressure field, a staggered grid is used. The solution algorithm can be summarized as follows

- Consider an initial guess for P and *V*.
- V^* is calculated using equation (12) which is composed of three scalar equations.
- Having V^*, pressure at new time step (P^{n+1}) is obtained by solving the Poisson equation (14) using the SOR method
- After determining P^{n+1} and V^*, V^{n+1} is obtained from the solution of equation (13) explicitly.
- Repeat steps 2 to 4 with V^{n+1} and P^{n+1} as new initial guesses until the convergence criterion is satisfied.

3 RESULTS AND DISCUSION

To validate the code implemented here, the curved pipe is set nearly close to the straight pipe by fixing a value of $\delta = 1\times10^{-5}$ for the curvature, and its axial velocity profile in the fully developed region is compared with the analytical solution of the fully developed velocity profile of the straight pipe in Fig. 5, indicating a good agreement. At the following, different features of the developing flow inside a curved pipe will be studied in detail and finally it will be focused on proposing a correlation to predict entrance length in the curved pipes.

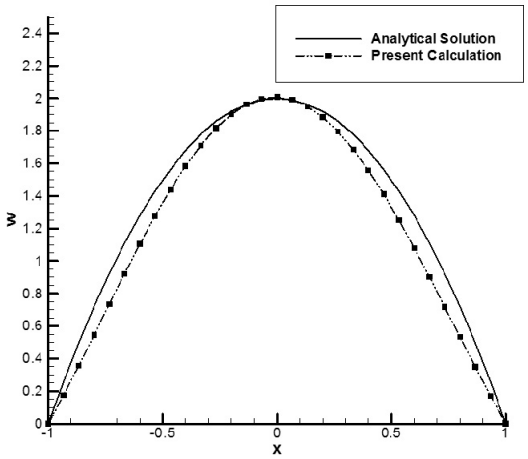

Figure 5. Comparison of axial velocity profile in fully developed region between present work at $\delta = 1\times10^{-5}$ and analytical solution for straight pipe

3.1 Axial velocity

The trend of developing of axial velocity on the symmetry plane has been shown in Fig. 6(a). Because of pipe curvature, centrifugal forces appear and cause the fully developed axial velocity profile to be different from that of the straight pipe. Hence as the flow progresses downstream in the curved pipe, due to centrifugal forces, boundary layer on the inner wall ($x = 1$) develops faster than the outer wall ($x = -1$) deviating maximum axial velocity from center line of the curved pipe toward the outer wall. This trend continues as fluid flow downstream, and ultimately at the fully developed region it approaches to the closest fixed point to the outer wall depending on the curvature and Reynolds number, where a steep velocity gradient near the outer wall presents. In Fig. 6(b), a three dimensional view of the axial velocity at the entrance region is illustrated to get a better perspective.

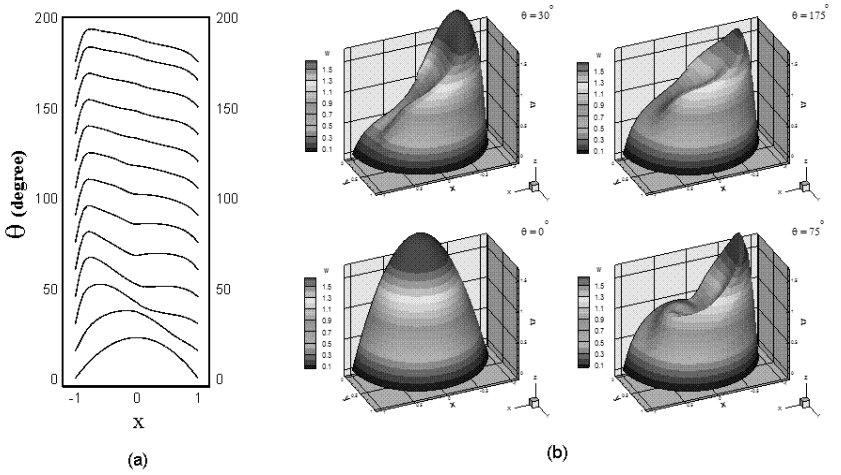

Figure 6. Development of the axial velocity profiles in the axial direction, δ=0.1 and Re=500
(a) on the symmetry plane (b) 3D shown in different sections

To better understand the developing pattern, the axial iso-velocity contours are shown in Fig. 7 at different sections. At the section of $\theta = 15°$, the parabolic profile of the inlet velocity has been partly conserved but beyond that the maximum velocity deviates toward the outer wall and deforms from the symmetrical profile. It can be easily observed that at the sections of $\theta = 45°$ and $60°$, double peaks appear (contour 1). Soh and Berger[4] have also reported this phenomenon.

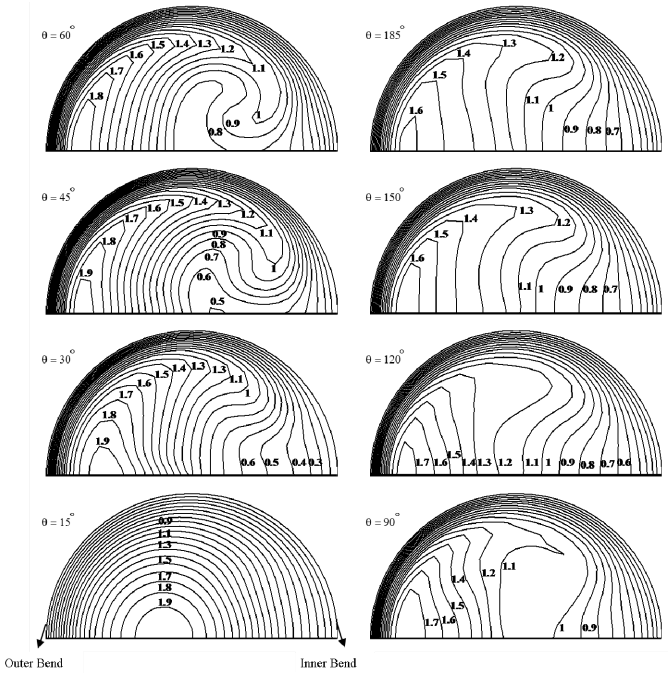

Figure 7. Contours of axial iso-velocity at different sections for δ=0.1 and Re=500

3.1 Secondary flow

Secondary flows in the stationary curved pipe develop due to centrifugal forces. At the very beginning of the entrance region, the strength of secondary flows are relatively high, but far downstream approaching to the fully developed region it weakens. This trend is shown in Fig. 8 where the secondary flow vector fields are plotted, indicating generation of vortices at different cross sections of the entrance region.

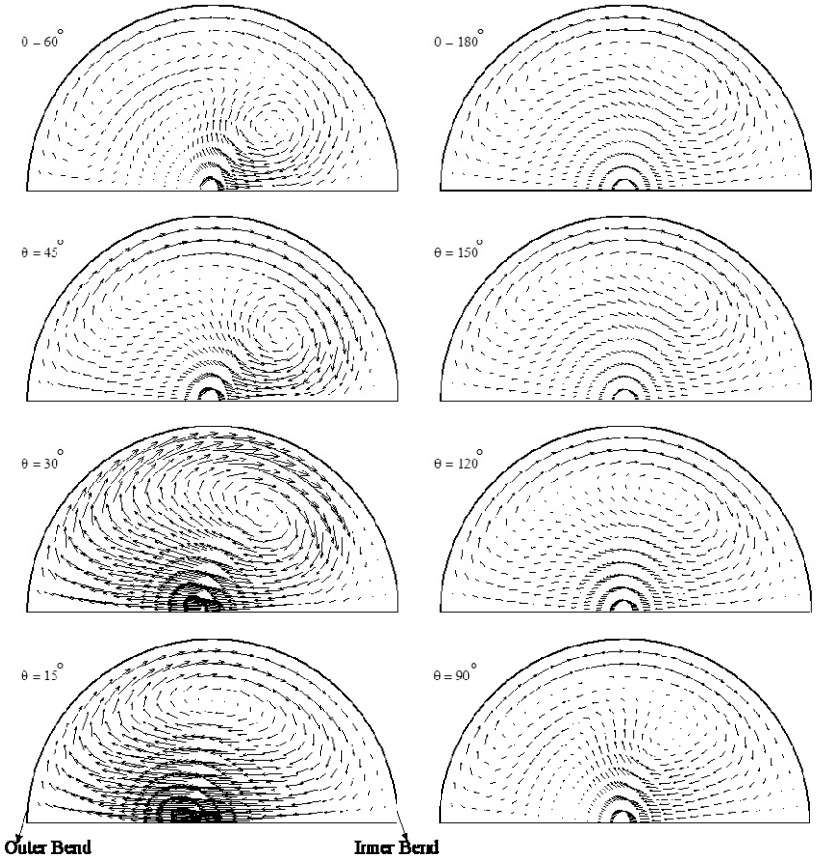

Figure 8. Vectors of secondary flow in different sections, δ=0.1 and Re=500.

A closer look at Fig. 6(a) reveals that the flow is almost reached to fully developed region at the section of $\theta = 175°$ and the axial velocity profile stays unchanged along the curved pipe axis. In this paper to capture the fully developed entrance length the following criterion is used

$$\frac{\partial w}{\partial \theta} = 0 \tag{16}$$

Table 1 shows the results for various combinations of δ and Re. In this table, the fully developed location is given in terms of angle θ and ratio *L/D* in which *L* is measured from the inlet of curved pipe along its center line. Using the above results obtained for 29 cases and utilizing the least square method, the following correlation to predict fully developed entrance length can be introduced in terms of δ and Re

$$\frac{l}{D} = 0.45814\ \mathrm{Re}^{0.42498}\ \delta^{-0.38334}$$

$$125 \le \mathrm{Re} \le 750 \quad \& \quad \frac{1}{30} \le \delta \le \frac{1}{10}$$

	Re	θ	*l/D*
δ = 1/10	125	95	8.290314
	250	140	12.2173
	375	165	14.39897
	500	175	15.27163
	625	185	16.1443
δ = 1/15	125	75	9.817477
	250	110	14.39897
	375	120	15.70796
	500	145	18.98046
	625	150	19.63495
	750	155	20.28945
δ = 1/20	125	65	11.34464
	250	90	15.70796
	375	105	18.32596
	500	120	20.94395
	625	125	21.81662
	750	135	23.56194
δ = 1/25	125	55	11.99914
	250	75	16.36246
	375	95	20.72578
	500	95	20.72578
	625	115	25.08911
	750	120	26.17994
δ = 1/30	125	50	13.08997
	250	60	15.70796
	375	85	22.25295
	500	90	23.56194
	625	100	26.17994
	750	110	28.79793

Table 1. Hydrodynamic fully developed length for different values of δ an Re

4 CONCLUSIONS

In this article, developing flow inside curved pipes is numerically studied using second order finite difference method based on the projection algorithm. The developing of the axial velocity and its dependence on the curvature and Reynolds number are investigated by illustrating the centrifugal effects due to the curvature in detail. Eventually, using numerous data obtained from the numerical simulation, a correlation is proposed to predict the entrance length in a curved pipe in terms of the curvature and the Reynolds number in a specified range.

REFERENCES

[1] Dean, W. R. (1927) "Note on the motion of fluid in a curved pipe" *Phil. Mag.* 20, 208
[2] Dean, W. R. (1928) "The streamline motion of fluid in a curved pipe" *Phil. Mag.* 30, 673
[3] Patankar, S. V., Pratap, V. S. & Spalding, D. B. (1974) "Prediction of laminar flow and heat transfer in helically coiled pipes" *J. Fluid Mech.* 62, 539
[4] Soh, W. Y. & Berger, S. A. (1984) "Laminar entrance flow in a curved pipe" *J. Fluid Mech.* 148, 109
[5] Agrawal, Y., Talbot, L. & Gong, K. (1978) "Laser anemometer study of flow development in curved circular pipes" *J. Fluid Mech.* 85, 497
[6] Kumar, Vimal & Nigam, K.D.P. (2005) "Numerical simulation of steady flow fields in coiled flow inverter" International Journal of Heat and Mass Transfer 48, 4811–4828
[7] Nobari, M.R.H., Gharali, K. (2006) "A numerical study of flow and heat transfer in internally finned rotating straight pipes and stationary curved pipes" International Journal of Heat and Mass Transfer 49, 1185–1194
[8] Yuan, S.W. (1967), *Foundations of Fluid Mechanics*, New Jersey: Prentice-Hall Inc.
[9] Hughes, W.F.; Gaylords, E.W. (1964), *Basic Equations of Engineering Science*, New York: Schaum.
[10] Aris, R. (1962), *Vectors, Tensors, and the Basic Equations of Fluid Mechanics*, Englewood Cliffs, N.J.: Prentice-Hall, Inc.
[11] Karamcheti, Krishnamurti (1967), *Vector Analysis & Cartesian Tensors: with Selected Applications*
[12] Ferziger, J.H.; Peric, M. (2002), *Coputational Method for Fluid Dynamics*, 3rd Ed., Berlin; New York; London: Springer